Magnetic Resonance Materials in Physics, Biology and Medicine (2024) 37:439–447
https://doi.org/10.1007/s10334-023-01129-4

RESEARCH ARTICLE

Improvement of image quality in diffusion-weighted imaging with model-based deep learning reconstruction for evaluations of the head and neck

Noriyuki Fujima[1] · Junichi Nakagawa[1] · Hiroyuki Kameda[2] · Yohei Ikebe[3,4] · Taisuke Harada[4] · Yukie Shimizu[1] · Nayuta Tsushima[5] · Satoshi Kano[5] · Akihiro Homma[5] · Jihun Kwon[6] · Masami Yoneyama[6] · Kohsuke Kudo[3,7,8]

Received: 15 July 2023 / Revised: 18 October 2023 / Accepted: 23 October 2023 / Published online: 21 November 2023

Abstract

Objectives To investigate the utility of deep learning (DL)-based image reconstruction using a model-based approach in head and neck diffusion-weighted imaging (DWI).

Materials and methods We retrospectively analyzed the cases of 41 patients who underwent head/neck DWI. The DWI in 25 patients demonstrated an untreated lesion. We performed qualitative and quantitative assessments in the DWI analyses with both deep learning (DL)- and conventional parallel imaging (PI)-based reconstructions. For the qualitative assessment, we visually evaluated the overall image quality, soft tissue conspicuity, degree of artifact(s), and lesion conspicuity based on a five-point system. In the quantitative assessment, we measured the signal-to-noise ratio (SNR) of the bilateral parotid glands, submandibular gland, the posterior muscle, and the lesion. We then calculated the contrast-to-noise ratio (CNR) between the lesion and the adjacent muscle.

Results Significant differences were observed in the qualitative analysis between the DWI with PI-based and DL-based reconstructions for all of the evaluation items ($p < 0.001$). In the quantitative analysis, significant differences in the SNR and CNR between the DWI with PI-based and DL-based reconstructions were observed for all of the evaluation items ($p = 0.002 \sim p < 0.001$).

Discussion DL-based image reconstruction with the model-based technique effectively provided sufficient image quality in head/neck DWI.

Keywords Deep learning · Diffusion magnetic resonance imaging · Neck · Image reconstruction

✉ Noriyuki Fujima
fujima@med.hokudai.ac.jp

[1] Department of Diagnostic and Interventional Radiology, Hokkaido University Hospital, N14 W5, Kita-Ku, Sapporo 060-8638, Japan

[2] Faculty of Dental Medicine Department of Radiology, Hokkaido University, N13 W7, Kita-Ku, Sapporo, Hokkaido 060-8586, Japan

[3] Department of Diagnostic Imaging, Graduate School of Medicine, Hokkaido University, N15 W7, Kita-Ku, Sapporo, Hokkaido 060-8638, Japan

[4] Center for Cause of Death Investigation, Faculty of Medicine, Hokkaido University, N15 W7, Kita-Ku, Sapporo, Hokkaido 060-8638, Japan

[5] Department of Otolaryngology-Head and Neck Surgery, Faculty of Medicine and Graduate School of Medicine, Hokkaido University, N15 W7, Kita Ku, Sapporo 060-8638, Japan

[6] Philips Japan, 3-37 Kohnan 2-Chome, Minato-Ku, Tokyo 108-8507, Japan

[7] Medical AI Research and Development Center, Hokkaido University Hospital, N14 W5, Kita-Ku, Sapporo, Hokkaido 060-8638, Japan

[8] Global Center for Biomedical Science and Engineering, Faculty of Medicine, Hokkaido University, N14 W5, Kita-Ku, Sapporo, Hokkaido 060-8638, Japan

Introduction

Diffusion-weighted imaging (DWI) is an important modality for evaluations of the head and neck due to its ability to detect lesions, differentiate between benign and malignant lesions, and predict treatment outcomes [1–4]. Single-shot echo-planar imaging (EPI) is the most commonly used readout technique [5], because single-shot EPI readout achieves rapid scanning with high signal acquisition. Moreover, the majority of magnetic resonance imaging (MRI) scanners support the implementation of the EPI sequence. Single-shot EPI nevertheless has significant drawbacks, including geometric image distortion resulting from the setting of a large number of EPI factors [6]. Image distortion may adversely impact the radiological diagnostic performance in image interpretation. The parallel imaging (PI) technique effectively reduces image distortion in EPI-based DWI by decreasing the number of EPI factors. However, increasing the reduction factor in PI leads to a decrease in the signal-to-noise ratio (SNR), accompanied by substantial image noise, particularly in areas with high geometry factors (g-factors) typically located at the center of the image [7]. Although increasing the number of excitations (NEX), i.e., multiple signal averaging, may reduce image noise and yield a sufficient SNR, doing so entails a longer scanning time. This extended duration may cause discomfort to patients and increase the likelihood of patient motion, which, in turn, lowers image quality. Additional supportive denoising techniques should, therefore, be explored to overcome these limitations.

Remarkable development has recently been achieved in the clinical application of deep learning (DL) with convolutional neural networks (CNNs) in the field of medical imaging [8–12]. Image reconstruction techniques based on DL in particular have demonstrated promising results in relation to denoising for the acquisition and reconstruction of MRI data [13–15]. One of the DL-based image reconstruction techniques, classified as 'model-based' processes, represent a leading-edge development in the domain of image denoising within MRI; these techniques have provided significant advancements in the field [16–19]. The model-based technique consists of a deep-learning architecture named Adaptive-compressed-sensing sensitivity-encoding (CS)-Net, which is a type of filtered U-net architecture, embedded inside the image reconstruction process. Due to its analytical framework, this model-based DL denoising approach capably manages a large amount of data derived from image acquisition and the reconstruction process, including signal information from individual channels in receiver coils as well as both magnitude and phase information. Consequently, the model-based DL method holds promise for the improvement of image quality, even in head and neck DWI, which typically contains considerable image noise.

We conducted the present study to assess the utility of a model-based DL image reconstruction by comparing with images reconstructed with the conventional PI-based method in head and neck DWI.

Materials and methods

Patients

The protocol of this retrospective study was approved by our institutional review board, and the requirement for patients' written informed consent was waived. Total 384 patients were referred to our hospital for the evaluation of the head and neck and underwent MR scanning during the period from April 2022 to November 2022. From these 384 patients, we selected the cases of 43 patients with the following inclusion criteria; (1) the patient underwent the scanning by a specific MR scanner equipped with the DL-based reconstruction function, and (2) the patient's MRI data set including DWIs with both the conventional PI- and DL-based reconstructions was available. Two of these 43 patients were excluded based on a failure to save the raw data of DWI for the image reconstruction. We analyzed the cases of the final total of 41 patients. Twenty-five of the 41 patients underwent pretreatment MR scanning for the evaluation of their head and neck tumor as an initial assessment. The other 16 patients underwent MR scanning for the evaluation after the treatment of their head and neck lesion as a follow-up examination. The process of patient selection is presented in Fig. 1. The characteristics of the 41 patients were as follows: 30 males and 11 females, median age 59 years (range 37–78 years). Among the 41 patients, the primary sites and the pathological diagnoses in the 25 patients who underwent pretreatment MRI for the initial evaluation of their primary tumors were as follows: pharyngeal squamous cell carcinoma (SCC) ($n=10$ patients), oral cavity SCC ($n=4$), nasal or sinonasal cavity SCC ($n=4$), sinonasal inverted papilloma ($n=1$), and parotid gland tumor ($n=6$). The other 16 patients were on follow-up status after the definitive treatment for their head and neck lesion (i.e., no lesions present). Patient characteristics are summarized in Table 1.

Imaging parameter

All scanning was performed using a 3.0-Tesla MR unit (Ingenia Elition; Philips Healthcare, Best, The Netherlands) with a 16-channel neurovascular coil. Two data sets of DWI with three orthogonal motion probing gradients were,

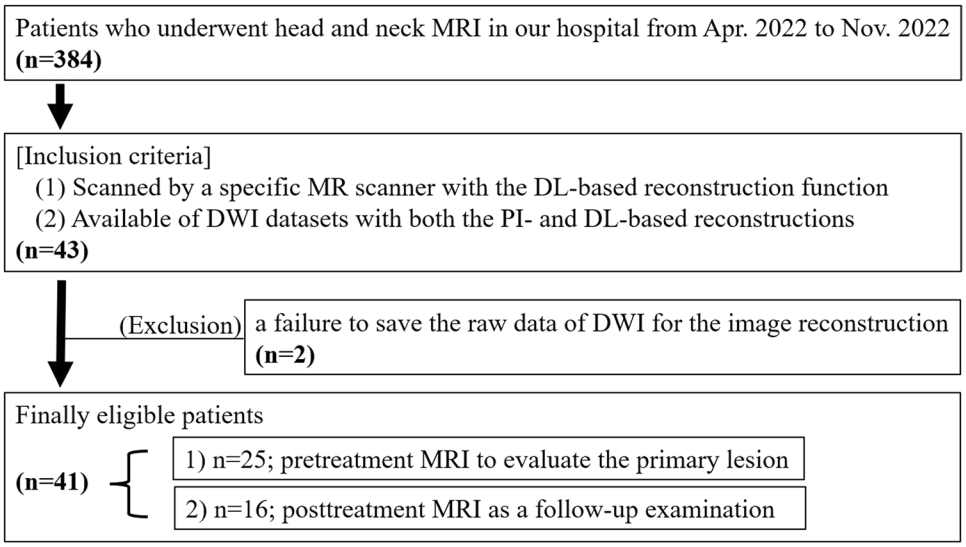

Fig. 1 Flow diagram of the study population. DL, deep learning; PI, parallel imaging; DWI, diffusion weighted imaging

Table 1 Patient characteristics ($n=41$)

Total patients (n = 41)	
Age	
Range	37–78
Median	59
Gender	
Male	30
Female	11
Detail of primary lesion (25 of 41 total patients)	
Pharyngeal SCC	10
Oral cavity SCC	4
Nasal or sinonasal cavity SCC	4
Sinonasal inverted papilloma	1
Parotid gland tumor	6

SCC, squamous cell carcinoma

respectively, acquired: (1) 2D single-shot spin-echo (SE) EPI-based DWI with PI reconstruction, and (2) 2D single-shot spin-echo EPI-based DWI with DL reconstruction. Two sets of DW images were thus obtained using the same image acquisition protocol with the following parameters: TR 4000 ms, TE 61 ms, flip angle 90°, EPI factor 45, acquired matrix 156 × 156 (reconstructed matrix, 256 × 256), field of view (FOV) 230 × 230 mm (matrix size 0.9 × 0.9 mm), slice thickness 5 mm, inter-slice gap 1.5 mm, reduction factor 3.0, number of excitations (NEX) 1, scanning time 1 min 1 s. The mean value derived from the three orthogonal directional DWIs was utilized for subsequent analyses.

Data processing

We used the image reconstruction model including the DL architecture of the Adaptive-CS-Net in retrieving the image from an undersampled k-space by the iterative image processing for the improvement of image quality; this method is classified as model-based DL reconstruction [16]. An overview of the iterative process in this model-based DL reconstruction is presented in Fig. 2. The details of the model training of Adaptive-CS-Net and of optimization methods are described in a previous report [16]. All image processing was conducted within the MR console.

This technique is used to achieve improved image quality from an undersampled k-space by iterative image processing by a DL-based image sparsifying approach mainly for denoising and removing artifacts with Adaptive-CS-Net. More specifically, Adaptive-CS-Net employs a CNN as a sparsifying transform, which serves to substantively replace the wavelet transform within the framework of the compressed sensing algorithm. Adaptive-CS-Net was constructed based on a U-Net-shaped structure with a soft thresholding function that could help achieve efficient image processing, such as denoising and removing artifacts. We speculated that, as a result of embedding Adaptive-CS-Net into an iterative processing of image reconstruction, more accurate image quality improvement could be expected by fully dealing with not only the final output images but also the substantial total amount of data processed iteratively through the Adaptive-CS-Net within the image reconstruction cycle. In addition, as another important characteristic of this model-based reconstruction process, we input the image reconstruction-related data set of domain-specific knowledge (e.g., data consistency, phase behavior, and background information) in the reconstruction process; the process for data consistency check makes it possible to avoid inappropriate processing by canceling the specific denoising/artifact reduction that is inconsistent with the original image data, the process for inputting the phase behavior was to remove the slowly varying phase caused by acquisition errors or

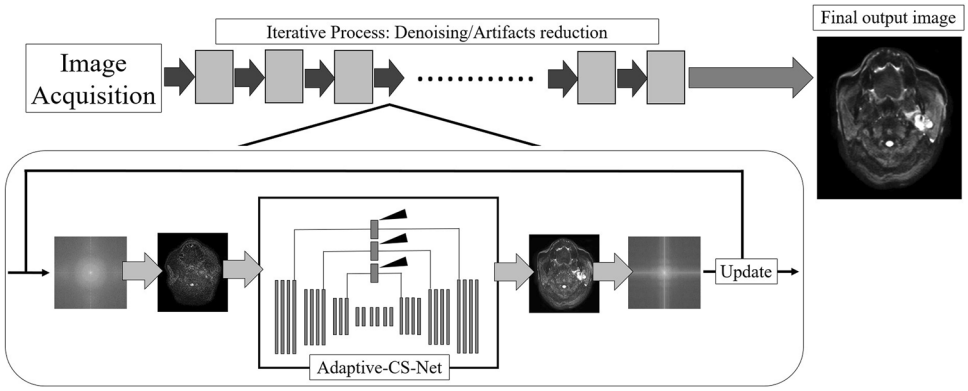

Fig. 2 Overview of the model-based deep learning (DL) reconstruction process. This schematic diagram shows the model-based DL reconstruction framework, which is characterized by the iterative processing by a DL-based image sparsifying approach. In this model, the deep learning architecture of Adaptive-CS-Net was embedded in the image reconstruction cycle. Adaptive-CS-Net is based on a U-Net-shaped structure, with a soft thresholding function (arrowheads). In the reconstruction process, image data undergo iterative processing with image sparsifying by Adaptive-CS-net. This process produces a final output image with high image quality

imperfections, and the process for inputting the background information was to estimate the coarse signal distribution in the FOV from low frequency k-space data. These processes lead to reliable background identification in the reconstruction process. [16, 17]. Finally, from a single set of acquired DWI data, a corresponding set of images was output through the model-based DL reconstruction process. Conventional PI-based DWI, which is the most frequently used DWI sequence, was compared with the above-described model-based DL reconstruction method.

Image analysis: qualitative assessment

As a qualitative assessment, two board-certified radiologists who are head-and-neck imaging specialists with 8 and 17 years of experience in radiology, respectively, visually evaluated the axial DW images with PI- and DL-based reconstruction in a blinded fashion, focusing on: (i) the overall image quality, (ii) soft tissue conspicuity, and (iii) the degree of the artifact in all 41 patients. In patients with a primary tumor ($n=25$), (iv) lesion conspicuity was also evaluated. Each evaluation was conducted based on a five-point grading system as follows: 1 point, very poor, unavailable for diagnostic use; 2 points, poor, but possible for diagnostic use; 3 points, moderate, acceptable for diagnostic use; 4 points, good, minimal limitations for diagnostic use; and 5 points, excellent, almost no limitations for diagnostic use.

Image analysis: quantitative assessment

In the quantitative assessment, the signal intensity of the bilateral parotid glands, submandibular gland, and the posterior neck muscle was measured in all 41 patients by placing a circular 100 mm^2 region of interest (ROI) in all patients [20]. The SNRs of the normal tissue (the parotid glands, the submandibular gland, and the posterior muscle) were measured as follows: the mean signal in the ROI/standard deviation (SD) of the signal in the ROI [21]. In the patients with a primary lesion ($n=25$), a free-hand ROI was manually placed on the tumor lesion. If the tumor extended into two or more slices, the slice in which the largest area of tumor was depicted was selected. Any area which was suggested to be necrosis, a cystic lesion, or vessel component was carefully excluded from the ROI. The SNRs of the lesion were measured by the same fashion as the normal tissue. Subsequently, the contrast-to-noise ratio (CNR) was determined as follows. An additional ROI was manually drawn on muscle adjacent to the tumor lesion, and the CNR was then calculated as the difference between the mean signal of the tumor lesion and the adjacent muscle ROI divided by the SD of the adjacent muscle's ROI [21]. Finally, the apparent diffusion coefficient (ADC) was calculated using the signal intensity of b0 and b1000 images in the tumor lesion ROI. All of the ROI placement procedures were performed first on the patient's PI-based DWI images, and then the ROI was copied on the patient's DL-based DWI. Manual correction of the copied ROI placement was performed as needed. The quantitative procedure was performed by an experienced radiologist with 17 years of experience.

Statistical analysis

Kappa statistics were used to determine the interobserver agreement for the qualitative analyses (0.00–0.20, poor; 0.21–0.40, fair; 0.41–0.60, moderate; 0.61–0.80, good; 0.81–1.00, excellent). Qualitative image scores were compared between the DWI with PI-based and DL-based reconstructions using the Wilcoxon signed-rank test. The SNRs of

the normal tissues (parotid glands, submandibular gland, and posterior muscle) and the tumor lesion, the CNRs, and the ADCs were, respectively, compared between the DWI with PI-based reconstruction and DWI with DL-based reconstruction using the paired *t* test, after the confirmation of the data's normal distribution by the Shapiro–Wilk test. A p value < 0.05 was considered significant. SPSS software (IBM, Armonk, NY) was used for all statistical analyses.

Results

In the qualitative analysis, significant differences were observed between the DWI with PI-based reconstruction and the DWI with DL-based reconstruction in all of the evaluation items. The results of the qualitative analysis are summarized in Table 2. The interobserver agreement in all of the qualitative analyses between the two board-certified radiologists was mostly good (Kappa score of 0.59–0.68).

In the quantitative analysis, the sizes of the ROIs for the delineation of tumor lesions were 387 ± 212 mm^2. After the Shapiro–Wilk test, all quantitative variables were confirmed its normal distribution. We observed significant differences in the SNR between the DWI with PI-based and DL-based reconstructions in all of the normal anatomical structures (right and left parotid gland, submandibular gland, and the posterior muscle) and tumor lesions. In the CNR assessment for tumor lesions, the CNR between the lesion and adjacent muscle in the DL-based DWI (17.1 ± 13.0) was significantly higher than that in the PI-based DWI (12.6 ± 10.6) ($p < 0.001$). The ADCs in the DL-based DWI ($0.85 \pm 0.07 \times 10^{-3}$ mm^2/s) tended to be slightly higher than those in the PI-based DWI ($0.83 \pm 0.07 \times 10^{-3}$ mm^2/s), but significance was not observed ($p = 0.31$). Table 3 provides the results of all the quantitative analyses.

Representative cases of DWI images with PI-based and DL-based image reconstruction are presented in Figs. 3 and 4. In addition, cases wherein the efficacy of the model-based DL reconstruction was deemed insufficient are presented in Supplementary Materials 1 and 2.

Discussion

Our results revealed that the model-based DL image reconstruction technique with Adaptive-CS-Net successfully improved the image quality in DWI compared to the conventional PI-based technique in both qualitative and quantitative assessments for evaluations of the head and neck. To the best of our knowledge, the present study provides the first report of an assessment of the utility of DL-based image processing in head and neck DWI. This image reconstruction technique may be a useful tool in daily clinical practice for the assessment of the head and neck by providing high

Table 2 Results of the qualitative assessment

	Reader 1			Reader 2			Kappa-score
	Parallel-imaging	Deep-learning	p value	Parallel-imaging	Deep-learning	p value	
Overall image quality	2.88 ± 0.47	3.85 ± 0.55	< 0.001	2.75 ± 0.51	3.91 ± 0.45	< 0.001	0.68
Soft tissue conspicuity	2.64 ± 0.69	3.58 ± 0.60	< 0.001	2.73 ± 0.51	3.85 ± 0.43	< 0.001	0.61
Degree of the artifact	2.55 ± 0.70	3.67 ± 0.72	< 0.001	2.73 ± 0.56	3.82 ± 0.57	< 0.001	0.59
Lesion conspicuity	2.88 ± 0.71	3.73 ± 0.60	< 0.001	2.80 ± 0.57	3.80 ± 0.40	< 0.001	0.65

Data are mean ± standard deviation

Table 3 Results of the quantitative assessment

		Parallel imaging	Deep learning	p value
SNR	Lesion	9.8 ± 2.3	12.0 ± 2.9	< 0.001
	Rt. Parotid gland	9.5 ± 2.8	11.2 ± 3.4	< 0.001
	Lt. Parotid gland	8.8 ± 3.2	10.5 ± 3.9	0.002
	Rt. Submandibular gland	7.3 ± 1.8	9.2 ± 2.2	< 0.001
	Lt. Submandibular gland	7.1 ± 2.0	8.7 ± 2.4	0.002
	Rt. Cervical muscle	7.0 ± 1.4	8.9 ± 1.5	< 0.001
	Lt. Cervical muscle	7.1 ± 1.7	8.2 ± 1.8	< 0.001
CNR	Lesion to adjacent muscle	12.6 ± 10.6	17.1 ± 13.0	< 0.001
ADC (10^{-3} mm^2/s)	Lesion	0.83 ± 0.07	0.85 ± 0.07	0.31

Data are mean ± standard deviation. SNR, signal to noise ratio; CNR, contrast to noise ratio; ADC, apparent

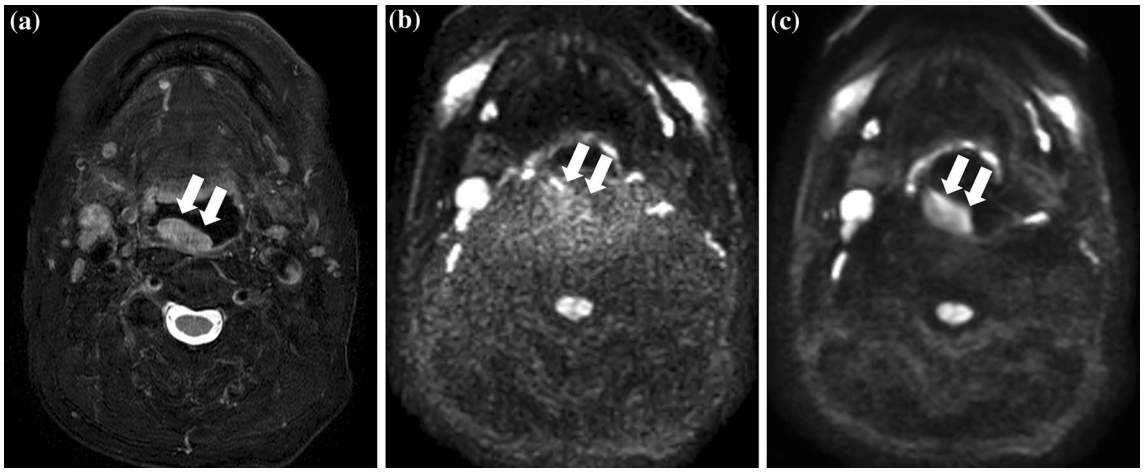

Fig. 3 Representative patient with posterior wall oropharyngeal cancer. In fat-suppressed T2WI (**a**), a primary tumor lesion located mainly on the posterior wall of the oropharynx was observed as a high-signal-intensity mass (a: arrow). In DWI with conventional PI-based reconstruction (**b**), the depiction of the primary lesion was unclear because of the bulk noise on the lesion (**b**: arrows). In contrast, the primary lesion was clearly depicted by the sufficient effect of noise reduction in DWI with the DL-based reconstruction (**c**: arrows)

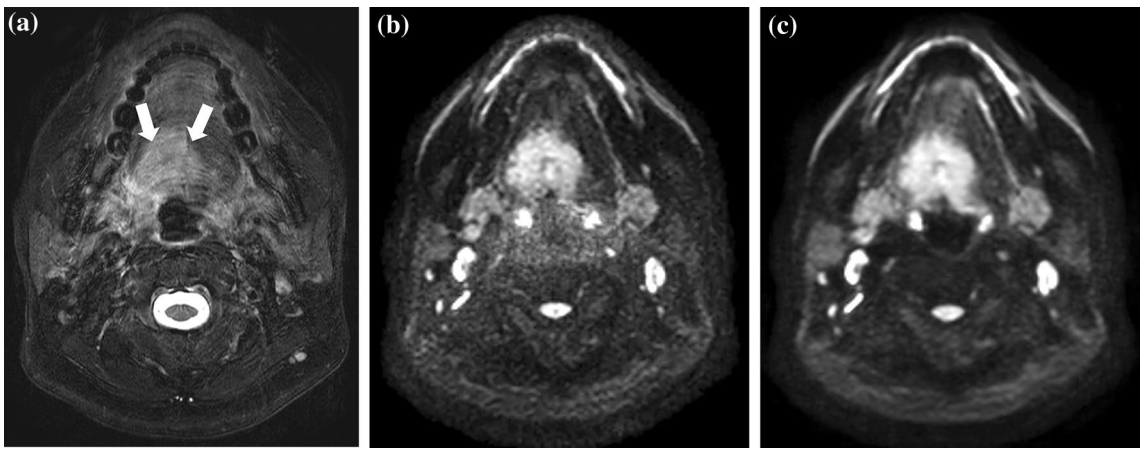

Fig. 4 Representative patient with cancer at the base of the tongue. Fat-suppressed T2WI indicated the tumor lesion on the base of the tongue (**a**: arrow). In DWI with conventional PI-based reconstruction (**b**), overall image noise was noticeable throughout the image (**b**); the depiction of normal anatomical structures as well as a part of the tumor was partially affected by image noise. In contrast, the DWI with DL-based reconstruction clearly depicted all of the normal structures and the lesion (**c**)

SNRs and CNRs with superb image visibility. We evaluated various tumor lesions, bilateral parotid glands, submandibular glands, and the posterior neck muscles for quantitative and qualitative assessments, and we observed that the image quality of all these targets was significantly improved. This result suggested that the model-based DL technique performed in this study achieved the overall favorable outcome in most of the locations in the head and neck. Regarding degree of artifact, B0 field inhomogeneity and EPI Nyquist ghost artifacts in DWIs frequently cause a decrease in image quality. The present results indicate that model-based deep DL reconstruction effectively decreases or eliminates a wide variety of artifacts or artifact-related noise and provides high-quality DWIs; however, it was unclear what kinds of artifacts were most or least effectively removed; further analysis is needed to clarify this issue.

In recent decades, conventional PI-DWI with single-shot SE-EPI has been a commonly used sequence design, and has frequently been applied for evaluations of the head and neck. However, the image acquisition of regions in the head and neck by conventional EPI-based DWI is often challenging because of its magnetic field inhomogeneity [22]; it can occasionally be difficult to maintain high image quality within an acceptable scanning time. Indeed, we

observed a certain degree of image noise in the PI-based DWI obtained in the present study. Koyasu et al. showed that readout-segmented EPI-based DWI significantly reduced the image distortion and provided more homogenous images compared to conventional single-shot spin-echo EPI [23]. As another readout technique, turbo spin-echo (TSE) DWI was also described as useful for evaluations of the head and neck [24]. These techniques may offer higher image quality; however, both sequence designs generally require a long scanning time. In addition, few scanners are available for such advanced sequences. In contrast, compared to conventional PI-based DWI, the DL-based reconstruction technique was found to successfully achieve effective improvement in image quality even in pixels with high g-factors by adopting a high-quality image processing strategy with Adaptive-CS-Net. This DL-based method is expected to play an important role in clinical practice for the evaluations of the head and neck. Recently, DWI processed with iterative denoising by a L1 regularization method such as wavelet transform has been introduced as a useful technique to obtain high-quality images [25]. We speculate that noise/artifact reduction by L1 regularization might be somewhat limited, because this technique is an algorithm-based method with a set threshold value in the wavelet transformation process; future comparison between this L1 regularization method and model-based DL reconstruction is needed.

DL-based image processing has been investigated in several prior studies on the acquisition of DWI for parts of the human body other than the head and neck [26–29]. Three of these prior studies in particular improved image quality using DL-based reconstruction without extending the acquisition time [26–28]. One of the previous studies utilized a DL-based reconstruction for DWI acquisition, which was performed using an end-to-end image-based DL technique targeting the prostate gland [26]. The other two studies were conducted to assess the usefulness of DL reconstruction utilizing the k-space-to-image method to assess the upper abdomen and breast [27, 28]. All of these previous studies have reported promising results, indicating that DL-based reconstructed DWIs show improved image quality. These existing DL-based methods have been considered clinically beneficial for image assessment using DWI. However, in these investigations, the output images with improved image quality were obtained mainly using CNNs that were trained for the conversion of output images (i.e., conversion from noisy images with under-sampled data to fully sampled images with good quality). Compared to this type of reconstruction method, which handles output images only, the model-based type of DL reconstruction used in the present study demonstrated an image processing using the Adaptive-CS-Net embedded in the iterative reconstruction cycle for effective denoising and removing artifacts. In this process, a large amount of signal data in the image reconstruction process can be well-utilized, handled, and integrated for effective image quality improvement while maintaining the data consistency [16, 30]. This method might achieve superior image quality compared to the post-processing type of DL-based method in which only output data sets (either of images or k-space data) are fed into a CNN. A prior study by Afat et al. conducted DL-based reconstruction for liver DWI using image processing with 17 unrolled iterations using raw k-space data as input [29]. Their method was somewhat similar to that used in the present study from the point of view that both investigations utilized the iterative technique in DL-based reconstruction. Their study focused on whether image quality could be maintained under a reduced scanning time using DL-based reconstruction. It would be interesting to assess to what extent image quality can be improved when the scanning time is not reduced, as in the present study.

Our study has several limitations. The number of patients was small ($n = 41$), because the study was conducted at a single institution. Our results should thus be regarded as preliminary. Second, each patient underwent two DWI scans for PI- and DL-based reconstruction. The differences between the two DWIs may also stem from variations in the acquisition conditions (e.g., accidental patient movement) and not solely from the reconstruction process. Third, we did not directly compare DWI with model-based-type DL image reconstruction with other DL-based reconstruction techniques. Although the model-based-type DL image processing was revealed to be more effective than that provided by the conventional PI-based technique, further investigations comparing several types of DL-based image processing are necessary to clarify this issue.

Conclusion

DL image reconstruction technique with a model-based approach successfully provided superb image quality in head and neck DWI and indicated superiority for denoising capability compared to the conventional PI-based method. This technique can be a useful tool for the assessment of patients with head and neck diseases.

Supplementary Information The online version contains supplementary material available at https://doi.org/10.1007/s10334-023-01129-4.

Acknowledgements This work was supported by a grant from the Japan Society for the Promotion of Science (JSPS) KAKENHI, No. JP21K07558.

Authors' contribution Fujima: study conception and design, acquisition of data, analysis and interpretation of data, drafting of manuscript. Nakagawa: acquisition of data, analysis and interpretation of data, critical revision. Kameda: acquisition of data, analysis and interpretation of data, critical revision. Ikebe: acquisition of data, analysis and interpretation of data, critical revision. Harada: acquisition of data, critical revision. Tsushima: acquisition of data, critical revision. Kano:

acquisition of data, critical revision. Homma: acquisition of data, critical revision. Kwon: analysis and interpretation of data, critical revision. Yoneyama: analysis and interpretation of data, critical revision. Kudo: study conception and design, critical revision.

Funding No funding was received for conducting this study. However, this work was supported by a grant from the Japan Society for the Promotion of Science (JSPS) KAKENHI, No. JP21K07558.

Data availability The data that support the findings of this study are not openly available due to reasons of sensitivity and are available from the corresponding author upon reasonable request.

Declarations

Conflict of interest Kwon Jihun and Masami Yoneyama are currently employed by Philips Japan. The other authors declare that they have no conflicts of interest.

Ethical approval All procedures performed in studies involving human participants were in accordance with the ethical standards of the institutional and/or national research committee and with the 1964 Helsinki declaration and its later amendments or comparable ethical standards. This study is retrospective, and the requirement for patients' written informed consent was waived.

Consent to participate The protocol of this retrospective study was approved by our institutional review board, and the requirement for patients' written informed consent was waived.

References

1. Thoeny HC, De Keyzer F, King AD (2012) Diffusion-weighted MR imaging in the head and neck. Radiology 263:19–32
2. Srinivasan A, Mohan S, Mukherji SK (2012) Biologic imaging of head and neck cancer: the present and the future. AJNR Am J Neuroradiol 33:586–594
3. Varoquaux A, Rager O, Dulguerov P, Burkhardt K, Ailianou A, Becker M (2015) Diffusion-weighted and PET/MR imaging after radiation therapy for malignant head and neck tumors. Radiographics 35:1502–1527
4. King AD, Thoeny HC (2016) Functional MRI for the prediction of treatment response in head and neck squamous cell carcinoma: potential and limitations. Cancer Imaging 16:23
5. Kolff-Gart AS, Pouwels PJW, Noij DP, Ljumanovic R, Vandecaveye V, de Keyzer F, de Bree R, de Graaf P, Knol DL, Castelijns JA (2015) Diffusion-weighted imaging of the head and neck in healthy subjects: reproducibility of ADC values in different MRI systems and repeat sessions. AJNR Am J Neuroradiol 36:384–390
6. Verhappen MH, Pouwels PJW, Ljumanovic R, van der Putten L, Knol DL, De Bree R, Castelijns JA (2012) Diffusion-weighted MR imaging in head and neck cancer: comparison between half-Fourier acquired single-shot turbo spin-echo and EPI techniques. AJNR Am J Neuroradiol 33:1239–1246
7. Yanasak NE, Kelly MJ (2014) MR imaging artifacts and parallel imaging techniques with calibration scanning: a new twist on old problems. Radiographics 34:532–548
8. Shen Y-T, Chen L, Yue W-W, Xu H-X (2021) Artificial intelligence in ultrasound. Eur J Radiol 139:109717
9. Laino ME, Viganò L, Ammirabile A, Lofino L, Generali E, Francone M, Lleo A, Saba L, Savevski V (2022) The added value of artificial intelligence to LI-RADS categorization: A systematic review. Eur J Radiol 150:110251
10. Kelly BS, Judge C, Bollard SM, Clifford SM, Healy GM, Aziz A, Mathur P, Islam S, Yeom KW, Lawlor A, Killeen RP (2022) Radiology artificial intelligence: a systematic review and evaluation of methods (RAISE). Eur Radiol 32:7998–8007
11. Barat M, Chassagnon G, Dohan A, Gaujoux S, Coriat R, Hoeffel C, Cassinotto C, Soyer P (2021) Artificial intelligence: a critical review of current applications in pancreatic imaging. Jpn J Radiol 39:514–523
12. Chassagnon G, De Margerie-Mellon C, Vakalopoulou M, Marini R, Hoang-Thi T-N, Revel M-P, Soyer P (2023) Artificial intelligence in lung cancer: current applications and perspectives. Jpn J Radiol 41:235–244
13. Mazurowski MA, Buda M, Saha A, Bashir MR (2019) Deep learning in radiology: An overview of the concepts and a survey of the state of the art with focus on MRI. J Magn Reson Imaging 49:939–954
14. Lin DJ, Johnson PM, Knoll F, Lui YW (2021) Artificial intelligence for MR image reconstruction: an overview for clinicians. J Magn Reson Imaging 53:1015–1028
15. Chaudhari AS, Sandino CM, Cole EK, Larson DB, Gold GE, Vasanawala SS, Lungren MP, Hargreaves BA, Langlotz CP (2021) Prospective deployment of deep learning in MRI: a framework for important considerations, challenges, and recommendations for best practices. J Magn Reson Imaging 54:357–371
16. Pezzotti N, Yousefi S, Elmahdy MS, Van Gemert JHF, Schuelke C, Doneva M, Nielsen T, Kastryulin S, Lelieveldt BPF, Van Osch MJP, De Weerdt E, Staring M (2020) An adaptive intelligence algorithm for undersampled knee MRI reconstruction. IEEE Access 8:204825–204838
17. Foreman SC, Neumann J, Han J, Harrasser N, Weiss K, Peeters JM, Karampinos DC, Makowski MR, Gersing AS, Woertler K (2022) Deep learning-based acceleration of compressed sense MR imaging of the ankle. Eur Radiol 32:8376–8385
18. Wu X, Tang L, Li W, He S, Yue X, Peng P, Wu T, Zhang X, Wu Z, He Y, Chen Y, Huang J, Sun J (2023) Feasibility of accelerated non-contrast-enhanced whole-heart bSSFP coronary MR angiography by deep learning-constrained compressed sensing. Eur Radiol. https://doi.org/10.1007/s00330-023-09740-8
19. Yang F, Pan X, Zhu K, Xiao Y, Yue X, Peng P, Zhang X, Huang J, Chen J, Yuan Y, Sun J (2022) Accelerated 3D high-resolution T2-weighted breast MRI with deep learning constrained compressed sensing, comparison with conventional T2-weighted sequence on 3.0 T. Eur J Radiol 156:110562
20. Hirata K, Nakaura T, Okuaki T, Kidoh M, Oda S, Utsunomiya D, Namimoto T, Kitajima M, Nakayama H, Yamashita Y (2018) Comparison of the image quality of turbo spin echo- and echo-planar diffusion-weighted images of the oral cavity. Medicine 97:e0447
21. Su T, Chen Y, Zhang Z, Zhu J, Liu W, Chen X, Zhang T, Zhu X, Qian T, Xu Z, Xue H, Jin Z (2020) Optimization of simultaneous multislice, readout-segmented echo planar imaging for accelerated diffusion-weighted imaging of the head and neck: a preliminary study. Acad Radiol 27:e245–e253
22. Avey G (2020) Technical improvements in head and neck mr imaging: at the cutting edge. Neuroimaging Clin N Am 30:295–309
23. Koyasu S, Iima M, Umeoka S, Morisawa N, Porter DA, Ito J, Le Bihan D, Togashi K (2014) The clinical utility of reduced-distortion readout-segmented echo-planar imaging in the head and neck region: initial experience. Eur Radiol 24:3088–3096
24. Mikayama R, Yabuuchi H, Sonoda S, Kobayashi K, Nagatomo K, Kimura M, Kawanami S, Kamitani T, Kumazawa S, Honda H (2018) Comparison of intravoxel incoherent motion diffusion-weighted imaging between turbo spin-echo and echo-planar imaging of the head and neck. Eur Radiol 28:316–324

25. Yoshida N, Nakaura T, Morita K, Yoneyama M, Tanoue S, Yokota Y, Uetani H, Nagayama Y, Kidoh M, Azuma M, Hirai T (2022) Echo planar imaging with compressed sensitivity encoding (EPICS): usefulness for head and neck diffusion-weighted MRI. Eur J Radiol 155:110489
26. Ueda T, Ohno Y, Yamamoto K, Murayama K, Ikedo M, Yui M, Hanamatsu S, Tanaka Y, Obama Y, Ikeda H, Toyama H (2022) Deep learning reconstruction of diffusion-weighted MRI improves image quality for prostatic imaging. Radiology 303:373–381
27. Bae SH, Hwang J, Hong SS, Lee EJ, Jeong J, Benkert T, Sung J, Arberet S (2022) Clinical feasibility of accelerated diffusion weighted imaging of the abdomen with deep learning reconstruction: comparison with conventional diffusion weighted imaging. Eur J Radiol 154:110428
28. Lee EJ, Chang Y-W, Sung JK, Thomas B (2022) Feasibility of deep learning k-space-to-image reconstruction for diffusion weighted imaging in patients with breast cancers: Focus on image quality and reduced scan time. Eur J Radiol 157:110608
29. Afat S, Herrmann J, Almansour H, Benkert T, Weiland E, Hölldobler T, Nikolaou K, Gassenmaier S (2023) Acquisition time reduction of diffusion-weighted liver imaging using deep learning image reconstruction. Diagn Interv Imaging 104:178–184
30. Knoll F, Murrell T, Sriram A, Yakubova N, Zbontar J, Rabbat M, Defazio A, Muckley MJ, Sodickson DK, Zitnick CL, Recht MP (2020) Advancing machine learning for MR image reconstruction with an open competition: overview of the 2019 fastMRI challenge. Magn Reson Med 84:3054–3070